ACTA
AMAZONICA

http://dx.doi.org/10.1590/1809-4392202502852

CHEMISTRY AND PHARMACOLOGY - ORIGINAL ARTICLE

Exploring chemical diversity in Amazonian *Vanilla* (Orchidaceae) through histochemistry and lipid profiling

Ianara Tamyres Fonseca BORGES[1], Ivoneide Maria Menezes BARRA[1,2], Felipe Fajardo Villela Antolin BARBERENA[1,3], Alberdan Silva SANTOS[2], Ana Carla FEIO[1,4]*

[1] Programa de Pós-graduação em Ciências Biológicas – Botânica Tropical (PPGBot), Universidade Federal Rural da Amazônia/Museu Paraense Emílio Goeldi, 66077-830, Belém, Pará, Brazil

[2] Universidade Federal do Pará, Laboratório de Investigação Sistemática em Biotecnologia e Biodiversidade Molecular, 66075-110, Belém, Pará, Brazil

[3] Universidade Federal do Rio de Janeiro, Núcleo de Pesquisas em Epífitas (Nupéfita), 27965-045, Macaé, Rio de Janeiro, Brazil

[4] Museu Paraense Emílio Goeldi, Campus de Pesquisa, Coordenação de Botânica, Laboratório de Anatomia Vegetal, 66077-830, Belém, Pará, Brazil

* Corresponding author: anacarlafeio@gmail.com

ABSTRACT

Vanilla is the most economically important genus of Orchidaceae due to the aromatic potential of some species, and comprises approximately 120 taxa. Lipid and phenolic compounds play key roles in flavor, aroma, antioxidant activity, and potential health benefits. This study compared the lipid and phenolic composition of leaves from two Amazonian *Vanilla* species, one of which is better documented, using chromatographic and infrared analyses integrated with *in situ* histochemical localization. Histochemical tests detected proteins, total phenolics, polysaccharides, mucilages, tannins, lipids, starch, alkaloids, and lignin in both species. Chromatographic analyses revealed 81 substances, of which 46 were identified: 31 common to both species, five exclusive to *V. labellopapillata*, and 10 exclusive to *V. pompona*. Infrared spectra showed high similarity between hexane extracts. This pioneering study, particularly for *V. labellopapillata*, demonstrates comparable metabolic and histochemical profiles, highlighting its potential for sustainable use and contributing to the valorization of Brazilian biodiversity.

KEYWORDS: Aroma; FTIR; Phenolic Compounds; *Vanilla labellopapillata*; *Vanilla pompona*

Explorando a diversidade química da baunilha amazônica (Orchidaceae) por meio de histoquímica e perfil lipídico

RESUMO

Vanilla é o gênero de Orchidaceae de maior importância econômica devido ao potencial aromático de algumas espécies e compreende aproximadamente 120 táxons. Compostos lipídicos e fenólicos desempenham papéis fundamentais em sabor, aroma, atividade antioxidante e potenciais benefícios à saúde. Este estudo comparou a composição lipídica e fenólica das folhas de duas espécies de *Vanilla* da Amazônia, uma das quais é mais bem documentada, utilizando análises cromatográficas e de infravermelho integradas à localização histoquímica *in situ*. Os testes histoquímicos detectaram proteínas, fenóis totais, polissacarídeos, mucilagens, taninos, lipídios, amido, alcaloides e lignina em ambas as espécies. As análises cromatográficas revelaram 81 substâncias, das quais 46 foram identificadas: 31 comuns a ambas as espécies, cinco exclusivas de *V. labellopapillata* e 10 exclusivas de *V. pompona*. Os espectros de infravermelho mostraram alta similaridade entre os extratos hexânicos. Este estudo pioneiro, em particular para *V. labellopapillata*, demonstra perfis metabólicos e histoquímicos comparáveis, destacando seu potencial para uso sustentável e contribuindo para a valorização da biodiversidade brasileira.

PALAVRAS-CHAVE: Aroma; FTIR; Compostos Fenólicos; *Vanilla labellopapillata*; *Vanilla pompona*

INTRODUCTION

The genus *Vanilla* Mill. comprises approximately 130 species distributed mainly in tropical regions of the world (Soto Arenas and Cribb 2010; Karremans *et al.* 2025). Brazil harbors the greatest diversity of the genus, with about 30 species, although the biochemical potential of many of them is still poorly explored (Silva *et al.* 2024; Meneguzzo 2025). Despite this knowledge gap, *Vanilla* is the orchid genus with the greatest economic value, mainly due to the production of natural vanilla extracted from the fruits of species such as *Vanilla planifolia* Andrews (Singletary 2020).

Phylogenetic studies indicate that American species, particularly those from Brazil and Central America, are closely related to *V. planifolia*. Species such as *Vanilla phaeantha*

CITE AS: Borges, I.T.F.; Barra, I.M.M.; Barberena, F.F.V.A.; Santos, A.S.; Feio, A.C. 2026. Exploring chemical diversity in Amazonian *Vanilla* (Orchidaceae) through histochemistry and lipid profiling. *Acta Amazonica* 56: e56cp25285.

Rchb.f. (syn. Vanilla bahiana Hoehne), *Vanilla chamissonis Klotzsh, and Vanilla pompona Schiede* form a clade with *Vanilla planifolia*, suggesting shared biosynthetic pathways involved in the production of valuable metabolites (Lopes et al. 2019; Karremans et al. 2025). Consequently, several *Vanilla* species have been investigated as alternatives for cultivation, genetic improvement, and as natural sources of bioactive compounds (Lopes *et al.* 2019; Silva Oliveira *et al.* 2025).

In this context, metabolomics represents a powerful high-throughput approach for the comprehensive analysis of metabolites, allowing the characterization of chemical profiles and metabolic networks, as well as comparisons between species and physiological conditions (Newgard 2026). In this study, untargeted lipid profiling was applied to lipid-enriched leaf extracts to profile known and unknown metabolites.

Most metabolomics studies in *Vanilla* have focused on the fruits, particularly on the identification of aromatic compounds such as vanillin, and on chemical variation related to domestication, environmental factors, and post-harvest processes (Cai *et al.* 2019; Silva *et al.* 2024). In contrast, the metabolomic characterization of the leaves remains underexplored, limiting our understanding of whole-plant metabolism and the potential of native and wild species as sources of novel bioactive compounds (Yu *et al.* 2021). Complementing metabolomic analyses, histochemical approaches allow the localization of metabolites in plant tissues, providing information about their morphofunctional roles and contributing to the interpretation of metabolic data (Babili *et al.* 2021; Athreya 2023). Phenolic compounds and lipids, for example, are directly associated with aroma, flavor, and the stabilization of sensory properties (Brillouet *et al.* 2010).

Vanilla pompona is recognized for its economic importance and has been extensively studied regarding the chemical composition of its fruits (Maruenda *et al.* 2013; Toth 2018). However, the chemical characterization of its leaves is still limited. In contrast, *Vanilla labellopapillata*, which is related to *Vanilla pompona* as both belong to the same subgenus, *Vanilla* subg. *Vanilla* (Karremans *et al.* 2025) have no published metabolomic or histochemical studies to date, representing a significant gap and an opportunity for biotechnological and taxonomic advancements. Therefore, the objectives of this study were to compare the chemical composition of *V. labellopapillata* and *V. pompona*, expand knowledge about the chemical composition of the genus, and analyze the spatial distribution of these compounds in the leaves and their possible morphofunctional roles.

MATERIAL AND METHODS

Collecting the botanical material

We selected *V. labellopapillata* (Collector nº: Borges 37; Borges 38; Borges 39 – Herbarium: MG 199985; 1° 25' 31.0" S 48° 25' 10.8" W) and *V. pompona* (Collector nº: Borges 40; Borges 41; Borges 42 – Herbarium: MG 234534; 1° 25' 31.9"S 48° 25' 10.0" W), two species that occur spontaneously in Utinga State Park, which is in the municipalities of Ananindeua and Belém, in Pará State. The collections of botanical material were carried out with authorization from the Institute for Forestry Development and Biodiversity of the State of Pará, process number 2023/991799. For each species, five fully developed leaves were collected from three individuals for the histochemical analyses. For the metabolomic analyses, we collected developed, healthy leaves (100 g of each species), with no apparent damage from phytopathogens and/or herbivores, which were separated, washed, and labeled in plastic bags.

Histochemical Characterization

The samples were fixed in FAA (formalin:acetic acid:ethanol 50%, 1:1:18, vol/vol; Johansen 1940) for 24 h, to structurally characterize them using light microscopy and to detect hydrophilic compounds, and in neutral buffered formalin for 24 h (NBF; Lillie 1965) to detect lipophilic compounds.

The leaf samples were dehydrated in a tert-butanol series, embedded in histological paraffin with DMSO (Paraplast®, Sigma-Aldrich), and sectioned (10–12 μm) with a semi-automatic rotary microtome (Leica®, RM 2245). Tests were performed to characterize the general histochemistry and detect lipids and phenolic compounds (active aromatic compounds responsible for the sensory characteristics of *Vanilla*), which act in stabilizing and amplifying the sensory properties in the fruits and may be present in the leaves as precursors of vanillin, respectively (Brillouet *et al.* 2010; Hernandéz-Fernandéz *et al.* 2020). For the general histochemistry characterization, the following tests were made: PAS (Periodic-Acid-Schiff's reagent) reaction for total polysaccharides (McManus 1948); ruthenium red (Gregory and Baas 1989) and tannic acid/ferric chloride (Pizzolato and Lillie 1973) to detect mucilages; Sudan Black B for total lipids (Pearse 1985); and Wagner reagent for starch and alkaloids (Furr and Mahlberg 1981). For the different phenolic classes, the following was used: 10% ferric chloride for total phenolic compounds (Johansen 1940); phloroglucinol for lignin (Johansen 1940); and vanillin/hydrochloric acid for tannins (Mace and Howell 1974). The control tests were made according to the respective protocols.

Obtaining the extracts

The leaf samples were dehydrated in a dryer with circulated and refreshed air, at 45º C, for twelve days. After complete dehydration, the material was manually ground and stored away from light and moisture. To obtain the crude extracts, extractions with solvents with different polarities: hexane for lipid extraction (Reis *et al.* 2021) and ethyl alcohol PA for the extraction of phenolic compounds (Reis *et al.* 2021) were made with the aid of ultrasound, at 45 ºC for 45 minutes. For each species, a single extraction was performed with each solvent, generating one analytical sample for each of the studied species. The metabolomic analysis methodologies were developed by the *Laboratório de Investigação Sistemática em Biotecnologia e*

Biodiversidade Molecular (LABSISBIO) at UFPA, under the supervision of Professor Dr. Alberdan Santos.

Transesterification method

For each sample, 10 mg of extract was transferred to a conical polypropylene tube with a snap cap, properly identified (TBx-A), to which 100 µL of 0.25 N KOH was added. Subsequently, the samples were agitated with a vortex mixer (Phoenix® AP59) and kept in an ultrasonic bath at 40°C for 10 min. After this, 700 µL of hexane was added and vortexed for approximately ten seconds. Distilled water was added to the extract, and the conical tubes with a volume of 2 mL were put in a centrifuge (Microhemato® Mod. 2410) for three minutes at 10,000 Rotation per minute (RPM). After centrifugation, the supernatants were transferred to another tube (TBx-B). A volume of 20 µL of 2N HCL was added into the first tube (TBx-A) and agitated in the vortex to acidify the sample. Subsequently, 600 µL of dichlorine-hexane (1:1) was added, and the samples were vortexed for ten seconds and then centrifuged for three minutes at 10,000 RPM. After centrifugation, the supernatants were transferred to the TBx-B. The sample residue (TBx-A) was submitted to evaporation to eliminate the residual water in a solvent evaporation automated system, and then derivatized.

Derivatization method

All samples were derivatized with N,O-bis-(trimethylsilyl) trifluoroacetamide (BSTFA) + 1% of trimetyl-chlorosilane (TMCS) to silylate the free molecules that were not transesterified. For the TBx-A tube, 50 mL of derivatized was added and kept in the ultrasonic bath at 60°C for 15 min. Then, it was cooled, and the transesterified lipids were transferred to the TBx-2 tube. Following this, the TBx-B tube was kept in the ultrasonic bath for 5 min, then centrifuged, and the supernatant content was put in a 2 mL glass vial with a cap and septum to be analyzed using GC/MS.

Thin Layer Chromatography (TLC) analysis

Hexane and ethanolic extracts of both species were applied as bands to 5 × 2.5 cm TLC plates (Aluminium, silica 60 mesh-fluorescence indicator 254 nm) using glass capillaries. Hexane extracts were eluted with hexane:ether:acetone (8:2 plus two drops of acetone), while ethanolic extracts were developed in chloroform:hexane:methanol (7:2.5:0.5). Plates were eluted in individual chambers and revealed using vanillin–sulfuric acid (VSA) as a universal reagent for lipid extracts (Reis *et al.* 2021). For the ethanolic extracts, we used the following developers: VSA (Reis *et al.* 2021), Draggendorff acid + tartaric acid, specific for alkaloids (Wagner and Bladt 2009) and diphenylboryloxyethylamine/polyethylene glycol (NP/PEG), specific for flavonoids and other phenolic compounds, resulting in yellowish, bluish, or greenish fluorescence under UV light at 365 nm (Wagner and Bladt 2009). All plates were visualized under UV light at 254 and 365 nm and analyzed following Wagner and Bladt (2009).

Gas chromatography–mass spectrometry (GC–MS)

The GC/MS analysis was done in a gas chromatograph (GC) with a self-sampler coupled to a Single Quadrupole mass spectrometer (MS). The GC was equipped with the capillary column ZB-5HT (5.00% Phenyl, 95.00% Dimethylpolysiloxane – 30 m length x 0.25 mm internal diameter; 0.10 mm film thickness). Helium was used as the carrier gas with a flow rate of 1mL/min, and 1.0 mL of the sample was injected in splitless mode. The injector operated at 250°C, and the oven's temperature programming started at 200°C. The temperature of the oven was raised until 300°C at a speed of 20°C/min and kept fixed for 10 min. The MS operated with an interface at 275°C, ionization source at 230° C, using a solvent's delay of 5 min and a mass range of 50-600 Da. The electronical ionization was 70 eV. The compound identifications were made by comparing the sample mass spectra with those in the NIST2011, WILEY2009, and FAMES2011 commercial libraries. The validation of retention time was made by calculating the retention indexes (Kovats index) from the homologous hydrocarbons mixture. The lipid concentration was calculated using the peak area normalization, represented as a ratio of each lipid species' peak area relative to the sum of all the detected peak areas (100%).

Fourier Transform Infra-Red (FTIR) Analysis

The FTIR analysis was conducted according to Rohman and Che Man (2013), with some modifications. The mid-infrared (MIR) spectroscopy analyses were conducted with a range of 650 to 4000 cm –1 using an FTIR Agilent Technologies spectrophotometer (CARY 630 FTIR, Santa Clara, CA, USA), equipped with an Attenuated Total Reflectance system (ATR) with a ZnSe crystal, and a deuterated triglycine sulfate (DTGS) detector. The resolution was 16 cm^{-1} with 32 scans. The volume of each oil sample was 20 µL. The ATR was cleaned with acetone, using a piece of cotton, and the depth correction was done automatically with air.

Statistical analysis and graphical representations

Only one sample per species was analyzed, highlighting variability among metabolites within each class. The lipidomic profiles of the species were assessed using the relative abundance (%) of 50 identified chemical compounds. Data preprocessing involved autoscaling to standardize contributions from major and minor compounds. Analyses included boxplots and heat maps, which illustrated the distribution of individual compound concentrations by chemical category for *V. labellopapillata* (Vlab) and *V. pompona* (Vpo). Each point represents a compound's relative concentration based on chromatographic peak areas.

Data analysis and visualization were conducted using the Gemini AI platform (Google, USA) as a computational interface to run algorithms in Python (version 3.x). Data processing and manipulation were performed using the Pandas library, and statistical and graphical analyses were performed using the Scikit-learn and Seaborn libraries.

RESULTS

In frontal view, both species have an adaxial epidermis with isodiametric cells, thickened and straight cell walls, whereas those of the abaxial surface are straight but elongated (Figure 1a-d). They present amphistomatic leaves, with stomata at the same level as the ordinary epidermis cells and anisocytic and tetracytic stomata (Figure 1e-h). In frontal view, *V. pompona* has only crystal raphides (Figure 1i), while *V. labellopapillata* has only prismatic crystals (Figure 1j).

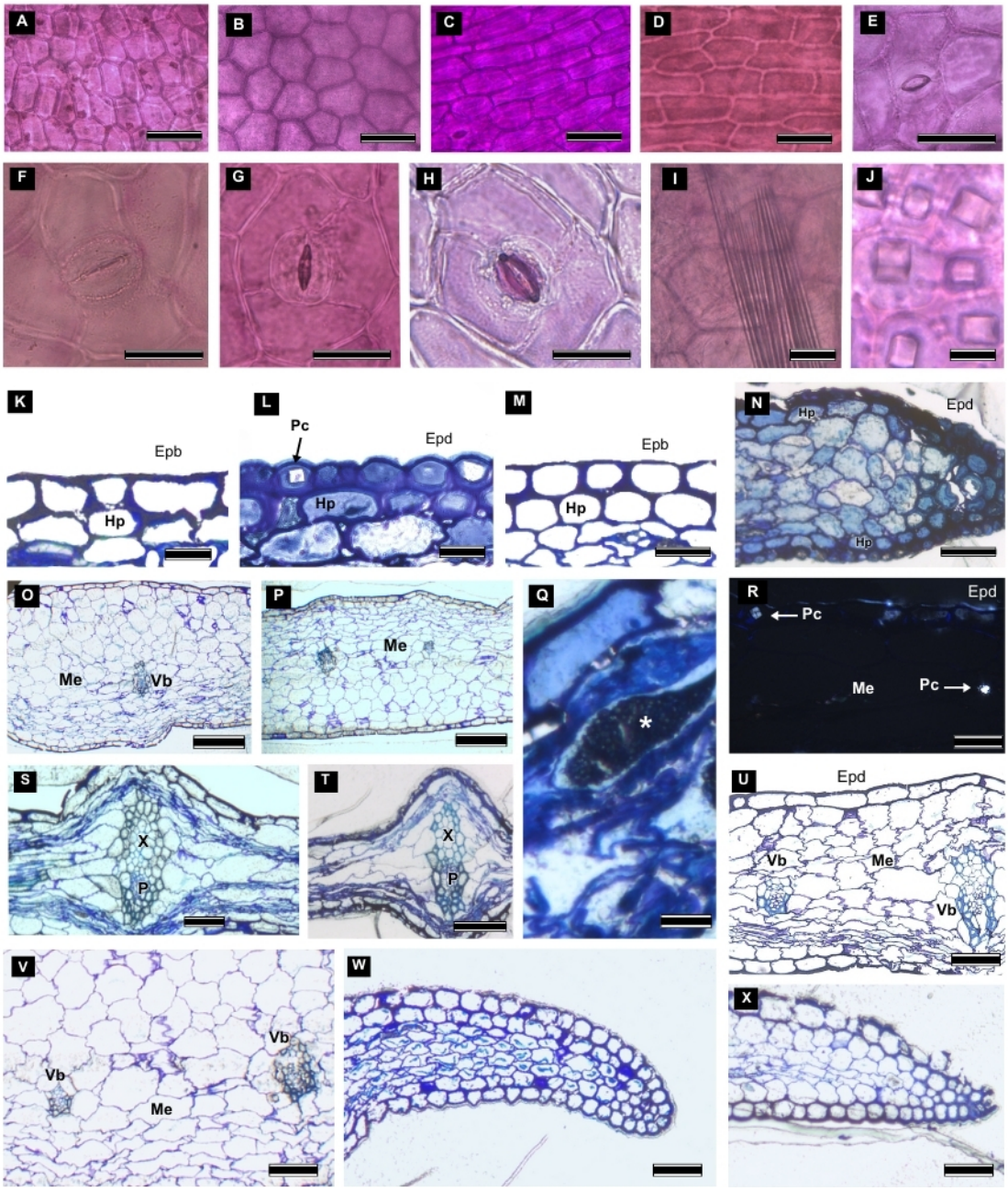


Figure 1. Anatomical leaf characterization of *Vanilla labellopapillata* and *Vanilla pompona* (A-J) Frontal view of the leaf epidermis. (K-X) Cross sections of the leaves. (A-B) Epidermic cells of the adaxial surface. (**A**) *V. labellopapillata*. (**B**) *V. pompona*. (C-D) Epidermic cells of the abaxial surface. (**C**) *V. labellopapillata*. (**D**) *V. pompona*. (E-F) Tetracytic stomata. (**E**) *V. labellopapillata*. (**F**) *V. pompona*. (G-H) Anisocytic stomata. (**G**) *V. labellopapillata*. (**H**) *V. pompona*. (**I**) Raphid crystals in *V. pompona*. (**J**) Prismatic crystals in *V. labellopapillata*. (K-L) Uniseriate epidermis and hypodermis. (**K**) *V. labellopapillata*. (**L**) *V. pompona*. (**M**) Hypodermis on the abaxial surface in *V. pompona*. (**N**) Hypodermis on the adaxial and abaxial surfaces in *V. labellopapillata*. (O-P) Homogeneous mesophyll. (**O**) *V. labellopapillata*. (**P**) *V. pompona*. (**Q**) Idioblasts with raphid crystals in *V. pompona*. (**R**) Crystals in the mesophyll and epidermis in *V. labellopapillata*. (**S**, **U**) Collateral vascular bundles in *V. labellopapillata*. (**T**, **V**) Collateral vascular bundles in *V. pompona*. (W-X) Revolute margins. (**W**) *V. labellopapillata*. (**X**) *V. labellopapillata*. Bars: (A-J) 50 µm; (K-X) 10 µm. Abbreviations: Epd = adaxial epidermis; Epb = abaxial epidermis; Vb = vascular bundle; Hp = hypodermis; Me = mesophyll; Pc = prismatic crystals; P = phloem; X = xylem.

In cross-section, both species present uniseriate epidermis, with isodiametric cells and thickened cell walls (Figure 1k-l). A parenchymatous, uniseriate hypodermis with elongated cells and thickened walls is present on the abaxial surface of *V. pompona*, and on both surfaces in *V. labellopapillata* (Figure 1m-n). The mesophyll, in both species, varies between 6-15 layers, is homogeneous, and the chlorenchyma has irregularly shaped cells with thin walls (Figure 1o-p). The cells are without conspicuous intercellular spaces. The presence of randomly distributed idioblasts with raphide crystals was observed in the mesophyll of *V. pompona* (Figure 1q), while in *V. labellopapillata* these crystals occur in the mesophyll and epidermis (Figure 1r).

Both species present collateral vascular bundles, with fibers associated with the phloem and xylem, arranged in parallel, alternating between large and small, in the median portion of the leaf blade (Figure 1s-v). In cross-section, the margins of the two species are revolute and consist solely of parenchymatous tissue (Figure 1w-x). Secretory idioblasts – an isolated secretory cell – were also observed in both species, scattered throughout the epidermis, mesophyll, and vascular bundles (Figure 2).

In situ histolocalization

The histochemical tests were positive in the idioblasts for both species, and proteins, total phenolic compounds, total polysaccharides, mucilages, tannins, lipids, starch, alkaloids, and lignins were detected (Figure 2). In the epidermal idioblasts, proteins, polysaccharides, mucilages, and tannins were detected. In the mesophyll, the hypodermic idioblasts present proteins and mucilages, while in the idioblasts of the parenchymal portion of the mesophyll, proteins, phenolic compounds, tannins, polysaccharides, starches, mucilages, and lipids were detected. However, in the idioblasts of the vascular bundles, proteins and tannins were identified, and lignin is composed in the cell wall of fibers.

Thin Layer Chromatography (TLC)

Different elution systems and visualization reagents revealed chromatographic bands with varying polarity and coloration, indicating chemical diversity. Hexane extracts showed a predominance of nonpolar to moderately polar metabolites, consistent with solvent affinity. Fluorescent bands visualized under UV light at 254 nm indicated the presence of conjugated compounds such as carotenoids (CA), lipids (LP), monoacylglycerols (MAG), triacylglycerols (TAG), and free fatty acids (FFA), which are characterized by unsaturated systems capable of absorbing radiation in the ultraviolet region (Figure 3a). The application of the vanillin–sulfuric acid (VAS) reagent enabled the visualization of multiple chromatographic bands, suggesting the presence of several classes of organic metabolites, including phospholipids (PL), monoacylglycerols (MAG), diacylglycerols (DAG), triacylglycerols (TAG), free fatty acids (FFA), carotenoids (CA), as well as steroids and terpenoids (ST–TP) (Figure 3b).

For the ethanolic extracts, the use of more polar elution systems allowed the separation of polar and moderately polar metabolites in both species (Figures 3c-e). Visualization with the diphenylboric acid 2-aminoethyl ester/polyethylene glycol (NP/PEG) reagent resulted in fluorescent bands exhibiting yellow to orange coloration under UV light at 365 nm, a pattern characteristic of flavonoids such as flavones and flavonols (Figure 3f).

The application of Dragendorff's reagent acidified with tartaric acid revealed brown-colored bands near the origin of

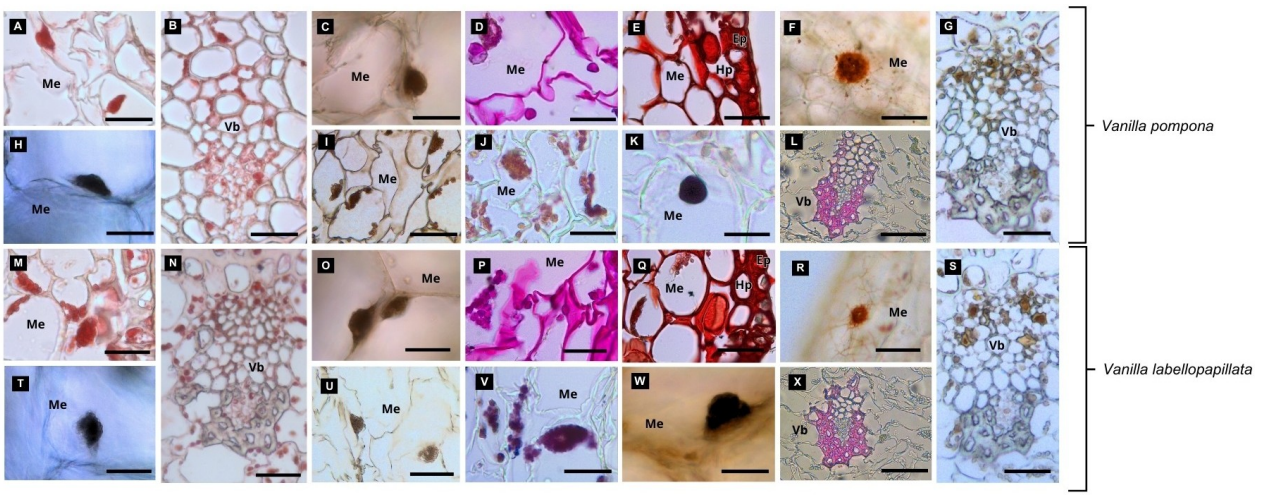


Figure 2. Positive histochemical results for the secretions of the secretory structures of *Vanilla pompona* (A-L) and *Vanilla labellopapillata* (M-X). (**A**, **B**, **M**, **N**) Xylidine test, proteins stained red. (**C**, **O**) Ferric chloride test, phenolic compounds stained brown. (**D**, **P**) PAS reaction test, polysaccharides stained pink. (**E**, **Q**) Ruthenium red test, mucilage stained pink. (**F**, **G**, **R**, **S**) Vanillin hydrochloric acid test, tannins stained reddish to brown. (**H**, **T**) Sudan Black test, lipids stained black. (**I**, **U**) Tannic acid and ferric chloride test, mucilage stained black. (**J**, **K**, **V**, **W**) Wagner reagent test, alkaloids stained from orange to reddish-brown, and starch stained black. (**L**, **X**) Phloroglucinol test, lignin stained pink to reddish. Bars: (A-T) 50 µm. Ep = epidermis; Vb = vascular bundle; Hp = hypodermis; Me = mesophyll.

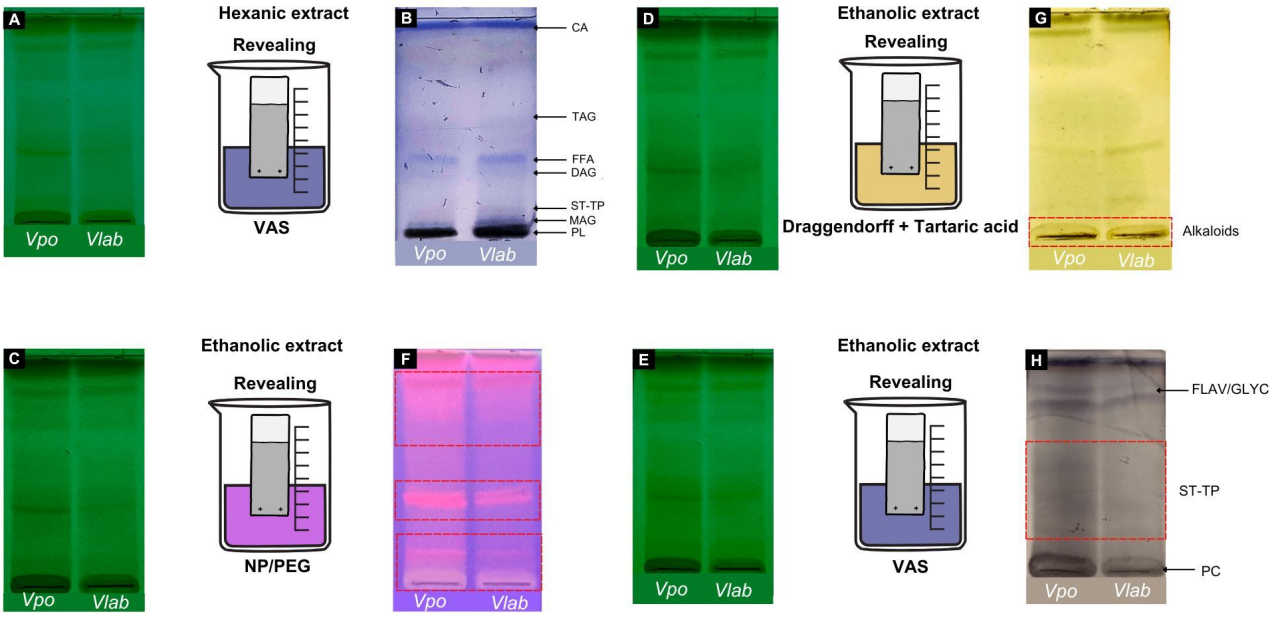


Figure 3. Thin-Layer Chromatography (TLC) of hexane and ethanolic extracts of *Vanilla labellopapillata* and *Vanilla pompona*. (A) Chromatoplate with hexane extracts after migration of an elution system visualized under 254 nm ultraviolet light. (B) Chromatoplate with hexane extracts after VSA development, visualized under visible light. (C-E) Chromatoplates with ethanolic extracts after migration of an elution system visualized under 254 nm ultraviolet light. (F) Chromatoplate with ethanolic extracts after NP/PEG development visualized under 365 nm ultraviolet light. (G) Chromatoplate with ethanolic extracts after development with Dragendorff + tartaric acid, visualized under visible light. (H) Chromatoplate with ethanolic extracts after development with VAS, visualized under visible light. Vlab: *Vanilla labellopapillata*; Vpo: *Vanilla pompona*. FFA: Free fatty acids; CA: Carotenoids; PC: Phenolic compounds; DGL: Diglycerol; ST-TP: Steroids and Terpenoids; PL: Phospholipids; FLAV: Flavonoids; GLYC: Glycosides; MAG: Monoacylglycerol; TAG: Triglycerides.

the chromatographic plate, indicative of the possible presence of alkaloids with low chromatographic mobility in more polar elution systems (Figure 3g). Additionally, visualization of the ethanolic extracts with VAS indicated the presence of phenolic compounds (PC), flavonoids, and/or flavonoid glycosides (FLAV-GLYC), as well as steroids and terpenoids (ST–TP) (Figure 3h).

Gas Chromatography–Mass Spectrometry (GC–MS)

Based on GC-MS analysis, a total of 81 substances were detected (40 in *V. labellopapillata* and 41 in *V. pompona*). For *V. labellopapillata*, 36 substances were identified (Table 1), of which three were the most concentrated (between 10–14%): substance 18 (Rt 32.08 - trimethylsilyl octadec-9-enoate), substance 12 (Rt 30.09 - methyl octadec-9-enoate), and substance 17 (Rt 31.98 - trimethylsilyl octadeca-9,12-dienoate) (Figure 4A). Other substances, such as 11 (Rt 29.97 - methyl octadeca-9,12-dienoate), 16 (Rt 31.5 - phytol TMS), 10 (Rt 29.15 - trimethylsilyl hexadecanoate), and 40 (Rt 45.2 – not identified, NI), had concentrations between 5–10%. The remaining substances detected had concentrations below 5%.

For *V. pompona*, 40 substances were identified (Table 1), of which four were the most concentrated (between 10–13%). The main substances identified were the following: 12 (Rt 30.11 - methyl octadec-9-enoate), 18 (Rt 32.07 - trimethylsilyl octadec-9-enoate), 11 (Rt 29.99 - methyl octadeca-9,12-dienoate), and 17 (Rt 31.98 - trimethylsilyl octadeca-9,12-dienoate) (Figure 4b). Three substances had intermediary concentrations, varying between 5% and 7%, including: 16 (Rt 31.48 - phytol TMS), 10 (Rt 29.17 - trimethylsilyl hexadecanoate), and 40 (Rt 45.17 - Dotriacosyl TMS ether (Derv). The remaining substances detected had concentrations below 5%.

Comparative FTIR analysis of chemical functional groups in *Vanilla* leaf extracts

For the infrared analysis, a general spectral similarity was observed between the hexanic extracts of *V. labellopapillata* (labeled as Vlab_hexane) and *V. pompona* (labeled as Vpo_hexane), with notable differences in spectral regions at 1625 cm^{-1}, 1390 cm^{-1}, 1260 cm^{-1}, 1050 cm^{-1}, and 850 cm^{-1} (Figure 5).

The band around 1625 cm^{-1} was observed in both hexane extracts and can be attributed to C=C stretching vibrations associated with unsaturated compounds, as well as, less specifically, to vibrations related to N–H bonds. The bands near 1390 cm^{-1} correspond to C–H bending vibrations, typical of methyl and methylene groups present in lipid structures. In the region of 1260 cm^{-1}, bands compatible with C–N or C–O stretching vibrations were observed, while the region around 1050 cm^{-1} is associated with C–C and C–O stretching vibrations, characteristic of long aliphatic chains and lipid esters (Stuart 2004).

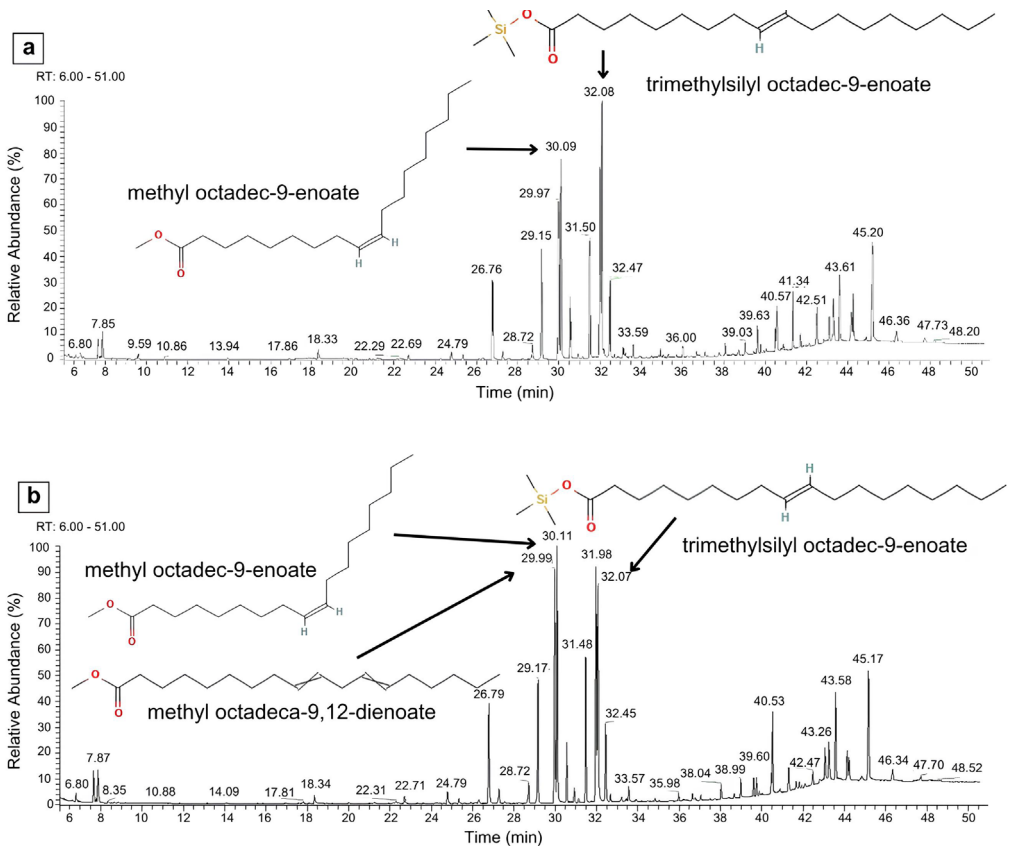


Figure 4. Gas chromatography-mass spectrometry (GC-MS) analysis of the leaves of *Vanilla labellopapillata* and *Vanilla pompona*. (A) Chromatogram of leaf extract of *V. labellopapillata*. (B) Chromatogram of leaf extract of *V. pompona*.

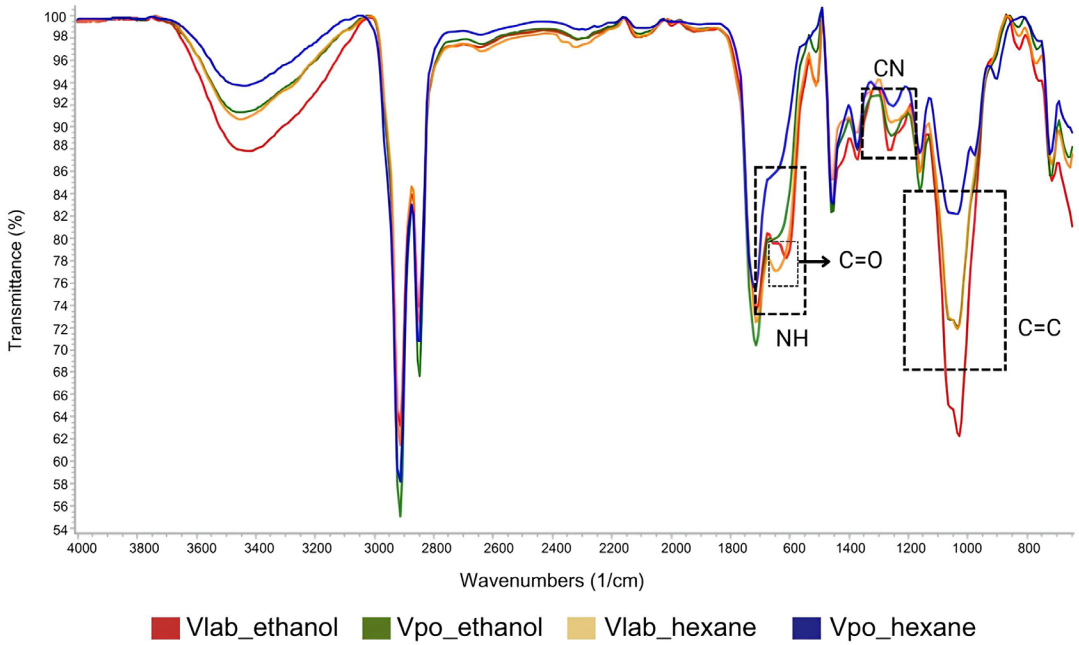


Figure 5. Fourier Transform Infra-Red (FTIR) analyses of the leaves of *Vanilla labellopapillata* and *Vanilla pompona*. Infrared spectra of hexane and ethanol extracts from the leaves of the two studied species. Vlab_ethanol: ethanolic extract of *V. labellopapillata*; Vpo_ethanol: ethanolic extract of *V. pompona*; Vlab_hexane: hexane extract of *V. labellopapillata*; Vpo_hexane: hexane extract of *V. pompona*.

Table 1. Chemical compounds identified in *Vanilla labellopapillata* and *Vanilla pompona* by means of gas chromatography-mass spectrometry (GC-MS) analysis. Rt: Retention time (in minutes); Vlab: *Vanilla labellopapillata*; Sd: Standard deviation; Vpo: *Vanilla pompona*; PC: Percentage concentration; NI: Not identified.

N	COMPOUNDS	Rt	PC Vlab %	Sd ±	PC Vpo %	Sd ±
1	Octyl TMS ether	9.59	0.24	0.02	-	0.00
2	Methyl decanoate	13.94	0.14	0.01	-	0.00
3	Methyl Dodecanoate	18.33	0.65	0.06	0.55	0.08
4	TMS dodecanoate	21.24	-	0.00	0.08	0.01
5	Methyl tetradecanoate	22.69	0.30	0.03	0.44	0.04
6	Methyl pentadecanoate	24.79	0.51	0.04	0.70	0.06
7	TMS tetradecanoate	25.34	0.25	0.02	0.28	0.03
8	Methyl hexadec-9-enoate	26.31	-	0.00	0.24	0.02
9	Methyl hexadecanoate	26.78	4.58	0.41	4,91	0.49
10	TMS pentadecanoate	27.28	0.42	0.03	0.81	0.08
11	Methyl heptadecanoate	28.72	0.79	0.08	1.08	0.09
12	TMS hexadecanoate	29.15	6.36	0.57	6.44	0.55
13	Methyl octadeca-9,12-dienoate	29.97	9.25	0.83	11.48	0.99
14	Methyl octadec-9-enoate	30.09	11.99	1.08	12.66	1.09
15	Methyl octadecanoate	30.56	3.03	0.18	2.65	0.23
16	TMS heptadecanoate	30.93	0.21	0.00	0.63	0.05
17	Octadecyl TMS ether	31.14	0.10	0.00	0.21	0.02
18	Phytol TMS	31.50	6.59	0.53	7.25	0.62
19	TMS octadeca-9,12-dienoate	31.98	10.73	0.97	10.37	0.89
20	TMS octadec-9-enoate	32.08	13.82	1.24	11.72	1.01
21	TMS octadecanoate	32.47	3.53	0.28	3.40	0.68
22	Farnesol TMS	32.69	-	0.00	0.29	0.02
23	Methyl 9,10-epoxyoctadecanoate	33.10	0.59	0.04	-	0.00
24	Methyl eicos-11-enoate	33.22	0.30	0.00	0.22	0.03
25	Methyl eicosanoate	33.59	0.60	0.05	0.61	0.05
26	Methyl heneicosanoate	34.83	-	0.00	0.13	0.01
27	NI	34.93	0.43	0.03	-	0.00
28	TMS eicosanoate	35.04	0.16	0.01	-	0.00
29	NI	35.29	0.17	0.00	-	0.00
30	Methyl docosanoate	35.98	0.49	0.01	0.30	0.24
31	2,3-bis[(TMS)oxy]prop-1-yl hexadecanoate	36.79	-	0.00	0.15	0.01
32	Methyl tricosanoate	37.07	0.20	0.02	0.20	0.03
33	Methyl tetracosanoate	38.07	0.50	0.05	0.57	0.14
34	Squalene	39.03	0.54	0.05	0.67	0.06
35	δ-Tocoferol TMS	39.76	0.44	0.04	0.71	0.06
36	Methyl hexacosanoate	39.9	-	0.00	0.18	0.04
37	γ-Tocoferol TMS	40.57	2.00	0.03	3.04	0.70
38	Octacosyl TMS ether	41.70	0.60	0.01	0.39	0.04
39	α-Tocoferol TMS	41.82	-	0.00	0.21	0.02
40	Cholesterol TMS	41.96	-	0.00	0.13	0.01
41	TMS octacosanoate	42.46	0.26	0.00	-	0.00
42	Nonacosyl TMS ether	42.51	1.47	0.02	0.57	0.07
43	Stigmasterol TMS	43.11	1.28	0.09	1.42	0.13
44	Triacosyl TMS ether	43.29	2.58	0.21	1.94	0.19
45	Sitosterol TMS	43.61	3.20	0.29	3.95	0.36
46	Hentriacosyl TMS ether (Derv)	44.18	1.76	0.12	1.59	0.35
47	NI	44.26	2.60	0.23	-	0.00
48	Dotriacosyl TMS ether (Derv)	45.17	-	0.00	6.05	1.51
49	NI	45.20	6.31	0.50	-	0.00
50	TMS dotriacotanoate	46.34	-	0.00	0.79	0.15

For the ethanolic extracts (identified as Vlab_ethanol and Vpo_ethanol), the spectra also showed high similarity, with a prominent band around 1600 cm^{-1}. In Vlab_ethanol, a possible double band in this region was observed, suggesting small variations in the relative composition of the metabolites (Stuart 2004).

Differences among species

Of the 46 compounds identified (Table 1), 31 occur in both species, 5 occur only in *V. labellopapillata*, and 10 only in *V. pompona*. Comparative analyses of the chemical categories reveal subtle, yet consistent, differences between *V. labellopapillata* and *V. pompona* regarding the derivatization pattern and overall lipid composition (Table 2).

Both species exhibited high variability in the TMS Derivatives (TMS) group, with compounds at high concentrations suggesting metabolic heterogeneity and marked accumulation of certain metabolites (Figure 6 a,b). The Methyl Ester (ME) group also showed wide distribution, with higher concentrations and dispersion in Vpo, indicating interspecific variations in lipid metabolism and fatty acid composition. For the TMS Ether/Alcohol (TMS-O) category, Vpo showed greater amplitude and higher concentrations than Vlab, suggesting superior abundance or diversity of these metabolites, while Vlab maintained lower average values and a narrow distribution.

The lipid heatmap revealed a similar overall metabolic profile between species, with only minor differences in relative abundance (Figure 6c). Variations mainly involved

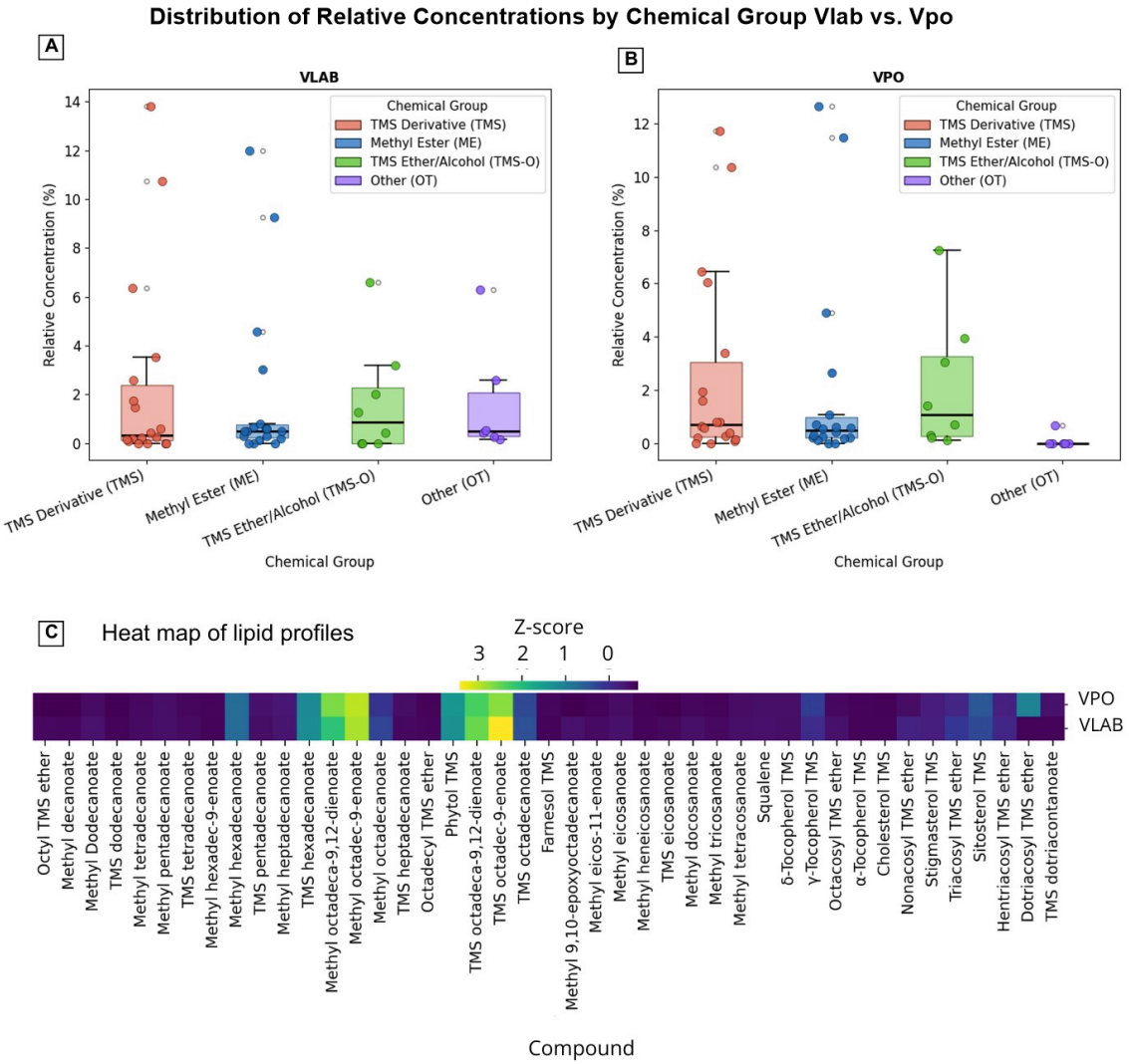


Figure 6. Distribution patterns of lipid profiles in the two species studied. (A-B) Distribution of relative metabolite concentrations by chemical category in *Vanilla labellopapillata* (A) and *Vanilla pompona* (B). Each point in the box plots represents the relative concentration (%) of an individual compound identified in its respective chemical group. (C) Comparative heat map of the lipid profiles of *Vanilla labellopapillata* and *Vanilla pompona*. The color scale on the right indicates the relative abundance of metabolites normalized by the Z-score, where shades of yellow/green represent lower intensity/relative concentration and shades of purple/dark represent higher intensity. Vlab: *Vanilla labellopapillata*; Vpo: *Vanilla pompona*.

Table 2. Percentage concentration of compounds distributed by chemical categories in *Vanilla labellopapillata* and *Vanilla pompona*. Sd: Standard deviation; Vlab: *Vanilla labellopapillata*; Vpo: *Vanilla pompona*.

Category	Species	Average	Sd	Total Vlab	Total Vpo	Discrimination Insight
ME (Methyl esters)	Vlab	2.15	3.86	33.32	36.32	Vpo exhibits greater esterification for common fatty acids.
	Vpo	2.19	4.09			
TMS (Trimethylsilyl)	Vlab	3.20	4.70	40.83	38.31	Vlab relies more on TMS esterification for C18 chains.
	Vpo	3.10	4.06			
TMS-O (Trimethylsilyl -Oxygenated Derivatives)	Vlab	2.70	2.41	13.07	16.87	Vpo is significantly richer in silylated sterols and tocopherols.
	Vpo	2.17	2.37			
OT (Others/ Not identified)	Vlab	2.41	2.75	10.05	0.67	Vlab contains more unidentified non-esterified (NI) components.
	Vpo	0.67	-			

unsaturated fatty acids and derivatives — especially methyl octadeca-9-enoate, methyl octadeca-9,12-dienoate, and their TMS derivatives — which were more abundant in *V. pompona*. Isoprenoid-derived metabolites (phytol TMS and farnesol TMS) also showed higher amounts in this species, whereas saturated fatty acids and sterols exhibited similar patterns in both species.

DISCUSSION

The histochemical analysis of *V. labellopapillata* and *V. pompona* leaves revealed a diversified secondary metabolic profile with a wide distribution of bioactive compounds in different tissues. The varied distribution of metabolites indicates specific morphofunctional adaptations in plant cells. In the idioblasts located within the epidermal cells, the presence of tannins, mucilages, and polysaccharides may serve multiple functions, including protection against herbivory and UV radiation, as well as regulating water loss, respectively (Tosif *et al*. 2021; Mendonça *et al*. 2025).

The presence of idioblasts with proteins and mucilage in hypodermal cells supports the idea that the hypodermis acts as a barrier for water storage and regulation, providing osmotic protection (Galloway *et al.* 2019; Nazari *et al.* 2022). The greater chemical diversity detected in mesophyll idioblasts (with lipids, phenols, starch, and mucilage), indicates that this tissue is not limited to photosynthesis but functions as a dynamic metabolic center (Busconi *et al.* 2017; He *et al.* 2020).

TLC analyses confirmed the broad metabolic diversity of the leaf extracts of *V. labellopapillata* and *V. pompona*, highlighting this technique as an effective qualitative phytochemical screening tool. The detection of bands consistent with phenolic compounds, terpenoids, and sterols agrees with previous reports for the genus *Vanilla* (Dignum *et al.* 2001; Palama *et al.* 2009). The predominance of nonpolar metabolites in hexanic extracts reflects the solvent's selectivity for lipophilic compounds, such as neutral lipids, carotenoids, and fatty acids (Harborne 1998; Reis *et al.* 2021). In contrast, ethanolic extracts preferentially revealed polar metabolites, including flavonoids and phenolic compounds, consistent with solvent polarity and NP/PEG TLC patterns (Wagner and Bladt 2009).

Further investigation of leaf phenolic compounds is needed to assess their aromatic potential, as the applied methods confirmed their presence in both species. Leaves may contain vanillin precursors and high concentrations of aromatic compounds, as reported for *Vanilla fragrans* (Baqueiro-Peña and Guerrero-Beltrán 2016). This suggests that vanillin biosynthesis may extend beyond fruits and that leaves of wild species may share biosynthetic mechanisms with commercial *Vanilla* species (Gallage *et al.* 2018).

The indicative detection of alkaloids, although not typical of the genus, was interpreted cautiously due to the qualitative nature of the method (Díaz-Bautista *et al.* 2018; Yusuf *et al.* 2023). Overall, TLC results complement GC–MS and FTIR analyses and reinforce the potential of *V. labellopapillata* and *V. pompona* as sources of secondary metabolites, supporting the integration of qualitative chromatography with advanced lipidomic approaches for chemical characterization of underexplored Amazonian species (Reis *et al.* 2021).

Chromatographic analyses revealed similar lipid profiles between the species, dominated by fatty acid esters and their trimethylsilyl derivatives, such as methyl octadec-9-enoate and trimethylsilyl octadec-9-enoate. These nonpolar lipids play key roles in stabilizing and transporting volatile aromatic compounds involved in vanilla aroma perception (Brillouet *et al.* 2010; Hernandéz-Fernandéz *et al.* 2020). Leaf lipid profiles reflect secondary metabolism, and the lipid similarity between the species suggests shared biosynthetic pathways and comparable aromatic potential, reinforcing the importance of organ-specific metabolic characterization, since the leaves of *V. planifolia* accumulate high levels of *Vanilla* precursors (Leyva *et al.* 2021; Beer *et al.* 2024).

According to the comparative analysis of the chemical categories, subtle yet consistent differences were observed between *V. labellopapillata* and *V. pompona* regarding the derivatization pattern and the overall lipid composition (Table 2). These differences, although not sufficient to clearly discriminate the species at a global level, indicate specific variations in the relative contribution of lipid classes and derivatized metabolites.

The distribution pattern of compounds observed for *V. labellopapillata* and *V. pompona*, marked by positive skewness, high variability, and outliers, is typical of biological datasets, especially in metabolomic and lipidomic studies. In such systems, most metabolites show low relative quantities, while a few contribute disproportionately to total variance, reflecting the dynamic and heterogeneous nature of biological systems and GC–MS–derived relative abundance data (Wörheide *et al.* 2021). Although *V. pompona* showed slightly higher dispersion and maximum substance values, the strong overlap of interquartile ranges and similar medians indicate no substantial difference between species. Such intra-experimental variability is common in complex biological studies influenced by physiological, environmental, and methodological factors (Blainey *et al.* 2014).

The differences in the quantities of compounds highlighted in the heat map, particularly for unsaturated fatty acids and their derivatives, may indicate metabolic adjustments related to desaturase activity, which regulates fatty acid unsaturation and membrane fluidity in plants (He and Ding 2020). The higher abundance of isoprenoid-derived metabolites, such as phytol TMS and farnesol TMS in *V. pompona*, may further reflect shifts in lipid metabolism linked to chlorophyll turnover and terpenoid pathways, with phytol serving as an indicator of tissue metabolic or physiological status (Lichtenthaler 1999). In contrast, the stability observed in the levels of saturated fatty acids and plant sterols between *V. labellopapillata* and *V. pompona* suggests conservation of membrane structural lipid fractions. Previous studies indicate that plant sterols, such as sitosterol and stigmasterol, act as stabilizing components of the lipid bilayer and exhibit lower metabolic plasticity compared to unsaturated fatty acids (Hartmann 1998; Schaller 2003).

The high similarity between the FTIR spectra from the hexane extracts suggests a general chemical profile dominated by nonpolar compounds, mainly neutral lipids. The bands associated with C–H (1390 cm^{-1}), C–O and C–C (1050–1260 cm^{-1}) vibrations are compatible with fatty acid esters, trimethylsilicates and other lipid metabolites, corroborating the GC-MS data. The band around 1625 cm^{-1} reinforces the predominance of unsaturated compounds, especially fatty acids, with its association with nitrogenous compounds being less likely, given the absence of complementary bands, in agreement with studies in plant lipid matrices (Bañuelos-Valenzuela *et al.* 2018). In ethanolic extracts, the band near 1600 cm^{-1} is typical of C=C vibrations of aromatic rings, indicating the predominance of phenolic compounds and flavonoids, common in extractions with polar solvents (Naumann 2000). Subtle variations observed between the spectra suggest relative differences in composition, without showing significant structural changes. Thus, the results confirm FTIR as an effective tool in chemical screening and comparison of metabolic profiles, acting in a complementary way to GC-MS and strengthening the chemical characterization of *V. labellopapillata* and *V. pompona* (Stuart 2004).

Beyond phylogenetic proximity, several *Vanilla* species, including *VV. chamissonis*, *V. phaeantha* and *V. pompona*, share biosynthetic pathways with *V. planifolia*, the main commercial species (Soto Arenas and Cribb 2010; Silva Oliveira *et al.* 2025). Because fruits and ovaries are evolutionarily homologous to leaves, comparative chemical studies are essential to expand vanilla genetic resources, particularly in light of increasing global demand and declining supply of natural vanilla (Bowman *et al.* 1999; Silva Oliveira *et al.* 2025). The chemical similarity observed suggests that *V. labellopapillata* has potential for commercial use, reinforcing its relevance as a sustainable, regionally adapted alternative for natural vanilla production. However, further studies on fruit chemistry and sensory properties are required to confirm this potential. Additionally, the leaves of *V. labellopapillata* and *V. pompona* exhibit promising agro-industrial potential due to their diverse bioactive compounds, including antioxidant and antimicrobial properties, which may be applied in bio-inputs, nutraceuticals, and cosmetic or pharmaceutical products (Januszewska *et al.* 2020; Andrew *et al.* 2024). Moreover, leaf biomass may be valorized as compost, biofertilizers, or agricultural substrates, promoting waste reduction and circular economy strategies, particularly relevant for the domestication and sustainable use of native *Vanilla* species such as *V. labellopapillata* (Divakaran *et al.* 2006; Lubinsky *et al.* 2008).

CONCLUSION

This is the first detailed study of the lipid and histochemical profile for *Vanilla labellopapillata*, an endemic species of the Amazon. *Vanilla labellopapillata* and *V. pompona* showed highly similar metabolic profiles, supporting further studies to expand the *Vanilla* gene pool amid increasing global demand. Although most compounds in *V. labellopapillata* occurred at low concentrations, they were biologically relevant, indicating the presence of potentially bioactive metabolites. The chemical similarity between species highlights *V. labellopapillata* as a promising candidate for sustainable vanilla production and reinforces its potential for conservation-oriented bioeconomy strategies.

ACKNOWLEDGEMENTS

The authors would like to thank the Plant Anatomy Laboratory at the *Museu Paraense Emílio Goeldi*, and the Systematic and Biotechnological Research and Molecular Biodiversity laboratories at the *Universidade Federal do Pará* (UFPA). Ianara Tamyres Fonseca Borges is grateful for the master's scholarship provided by the *Coordenação de Aperfeiçoamento de Pessoal de Nível Superior* (CAPES). This study was funded by the CAPES – Financial Code 001. Ana Carla Feio is grateful for the senior postdoctoral scholarship provided by *Fundação Carlos Chagas Filho de Amparo à Pesquisa do Estado do Rio de Janeiro* (FAPERJ/E26/203.422/2023).

REFERENCES

Andrew, E.; Etinagbedia, A.; Emakunu, S. 2024. Phytochemical constituents and bioactivities of *Hippeastrum puniceum*: A review. *International Journal of Science and Research Archive* 13:1314-1321.

Athreya, S. 2023. Histochemical staining of plant tissues. *International Journal for Multidisciplinary Research* 5:1-21.

Babili, E.; Rey-Rigaud, G.; Rozon, H.; Halova-Lajoie, B. 2021. State of knowledge: Histolocalisation in phytochemical study of medicinal plants. *Fitoterapia* 150:104862.

Bañuelos-Valenzuela, R.; Delgadillo-Ruiz, L.; Echavarría-Cháirez, F.; Delgadillo-Ruiz, O.; Meza-López, C. 2018. Composición química y FTIR de extractos etanólicos de *Larrea tridentata*, *Origanum vulgare*, *Artemisa ludoviciana* y *Ruta graveolens*. *Agrociencia* 52: 309-321.

Baqueiro-Peña, I.; Guerrero-Beltrán, J.A. 2016. *Vanilla* (*Vanilla planifolia* Andr.), its residues and other industrial by-products for recovering high value flavor molecules: A review. *Journal of Applied Research on Medicinal and Aromatic Plants* 6: 2214-7861.

Beer, F.; Weinert, C.H.; Wellmann, J.; Hillebrand, S.; Ley, J.P.; Soukup, S.T.; *et al.* 2024. Comprehensive metabolome characterization of leaves, internodes, and aerial roots of *Vanilla planifolia* by untargeted LC–MS and GC×GC–MS. *Phytochemical Analysis* 36: 1-22.

Blainey, P.; Krzywinski, M.; Altman, N. 2014. Points of significance: Replication. *Nature Methods* 11: 879-880.

Bowman J.L.; Baum S.F.; Eshed Y.; Putterill J.; Alvarez J. 1999. Molecular genetics of gynoecium development in *Arabidopsis*. *Current Topics in Developmental Biology* 454: 155-205.

Brillouet, J.; Odoux, E.; Conéjéro, G. 2010. A set of data on green, ripening and senescent vanilla pod (*Vanilla planifolia*: Orchidaceae): anatomy, enzymes, phenolics and lipids. *Fruits* 65: 221-235.

Busconi, M.; Lucini, L.; Soffritti, G.; Bernardi, J.; Bernardo, L.; Brunschwig, C.; *et al.* 2017. Phenolic profiling for traceability of *Vanilla* × *tahitensis*. *Frontiers in Plant Science* 8: 1-16.

Cai, Y.; Gu, F.; Hong, Y.; Chen, Y.; Xu, F.; An, K. 2019. Metabolite transformation and enzyme activities of Hainan vanilla beans during curing to improve flavor formation. *Molecules* 24:2-15.

Díaz-Bautista, M.; Francisco-Ambrosio, G.; Espinoza-Pérez, J.; Barrales-Cureño, H.; Reyes, C.; Herrera-Cabrera, B.; Soto-Hernández, M. 2018. Morphological and phytochemical data of *Vanilla* species in Mexico. Data in Brief 20: 1730-1738.

Dignum, M.J.W.; Kerler, J.; Verpoorte, R. 2001. *Vanilla* production: technological, chemical, and biosynthetic aspects. *Food Reviews International* 17: 199-219.

Divakaran, M.; Babu, K.N.; Peter, K.V. 2006. Conservation of vanilla species: A review. *Plant Genetic Resources* 4: 120-131.

Furr, Y.; Mahlberg, P.G. 1981. Histochemical analysis of laticifers and glandular trichomes in *Cannabis sativa*. *Journal of Natural Products* 44: 153-159.

Gallage, N.J.; Jorgensen, K.; Janfelt, C.; Nielsen, A.J.Z.; Naake, T.; Dunski, E.; *et al.* 2018. The intracellular localization of the vanillin biosynthetic machinery in pods of *Vanilla planifolia*. *Plant and Cell Physiology* 59: 304-318.

Galloway, A.; Knox, P.; Krause, K. 2019. Sticky mucilages and exudates of plants: Putative microenvironmental design elements with biotechnological value. *New Phytologist* 225: 1461-1469.

Gregory, M.; Baas, P. 1989. A survey of mucilage cells in vegetative organs of the dicotyledons. *Israel Journal of Botany* 38: 125-174.

He, C.; Liu, X.; Da Silva, J.; Liu, N.; Zhang, M.; Duan, J. 2020. Transcriptome sequencing and metabolite profiling analyses provide comprehensive insight into molecular mechanisms of flower development in *Dendrobium officinale* (Orchidaceae). *Plant Molecular Biology* 104: 529-548.

He, M.; Ding, N.Z. 2020. Plant unsaturated fatty acids: Multiple roles in stress response. Frontiers in Plant Science 11: 562785.

Harborne, J.B. 1998. *Phytochemical Methods: A Guide to Modern Techniques of Plant Analysis.* 3rd ed. Chapman & Hall, London. 302p.

Hartmann, M.A. 1998. Plant sterols and the membrane environment. *Trends in Plant Science* 3: 170-175.

Hernández-Fernández, M.Á.; García-Pinilla, S.; Ocampo-Salinas, O.I.; Gutiérrez-López, G.F.; Hernández-Sánchez, H.; Cornejo-Mazón, M. *et al.* 2020. Microencapsulation of vanilla oleoresin (*V. planifolia* Andrews) by complex coacervation and spray drying: physicochemical and microstructural characterization. *Foods* 9: 1375.

Januszewska, R.; Giret, E.; Clement, F.; Van Leuven, I.; Goncalves, C.; Vladislavleva, E.; *et al.* 2020. Impact of vanilla origins on sensory characteristics of chocolate. *Food Research International* 137: 109313.

Johansen, D.A. 1940. *Plant Microtechnique*. McGraw-Hill, New York. 523p.

Karremans, A.P.; Pupulin, F.; Damián-Parizaca, A. 2025. A revised infrageneric classification of *Vanilla* (Orchidaceae) based on phylogenetic, morphological and biogeographical evidence. *Phytotaxa* 715: 207-228.

Leyva, V.E.; Lopez, J.M.; Zevallos-Ventura, A.; Cabrera, R.; Cañari-Chumpitaz, C.; Toubiana, D.; *et al.* 2021. NMR-based leaf metabolic profiling of *V. planifolia* and three endemic *Vanilla* species from the Peruvian Amazon. *Food Chemistry* 358: 129365.

Lichtenthaler, H.K. 1999. The 1-deoxy-D-xylulose-5-phosphate pathway of isoprenoid biosynthesis. *Annual Review of Plant Physiology and Plant Molecular Biology* 50: 47-65.

Lillie, R.D. 1965. *Histologic Technic and Practical Histochemistry*, 3rd ed. McGraw-Hill, New York. 715p.

Lopes, E.M.; Linhares, R.G.; De Oliveira Pires, L.; Castro, R.N.; Souza, G.H.M.F.; Koblitz, M.G.B.; *et al*. 2019. *Vanilla bahiana*, a contribution from the Atlantic Forest biodiversity for the production of vanilla: A proteomic approach through high-definition nanoLC/MS. *Food Research International* 120: 148-156.

Lubinsky, P.; Bory, S.; Hernández, J.H.; Kim, S.C.; Gómez-Pompa, A.; Van Damme, P. 2008. Geographic dispersal of *Vanilla planifolia* and the origin of the Mexican vanilla industry. *Economic Botany* 62: 127-138.

Mace, M.E.; Howell, C.R. 1974. Histochemistry and identification of condensed tannin precursor in roots of cotton seedlings. *Phytopathology* 64: 1297-1302.

Maruenda, H.; Del Lujan Vico, M.; Householder, J.E.; Janovec, J.P.; Cañari, C.; Naka, A.; *et al.* 2013. Exploration of *Vanilla pompona* from the Peruvian Amazon as a potential source of vanilla essence: Quantification of phenolics by HPLC-DAD. *Food Chemistry* 138: 161-167.

McManus, J.F. 1948. Histological and histochemical uses of periodic acid. *Stain Technology* 23: 99-108.

Mendonça, R.A.; Farias, R.P.; Feio, A.C. 2025. Comparative anatomy with emphasis on the functional role of leaf secretory structures in herbivory resistance of two coexisting *Microgramma* species (Polypodiaceae). *New Zealand Journal of Botany* 65: 1253 - 1267.

Meneguzzo, T.E.C. 2025. *Vanilla* in Flora and Funga do Brasil. Jardim Botânico do Rio de Janeiro. (https://floradobrasil.jbrj.gov.br/FB12347). Acessed on 28 Aug 2025.

Naumann, D. 2000. Infrared Spectroscopy in Microbiology. In Encyclopedia of Analytical Chemistry (ed. R.A. Meyers), Wiley: Chichester, UK.

Nazari, M.; Bickel, S.; Benard, P.; Mason-Jones, K.; Carminati, A.; Dippold, M. 2022. Biogels in soils: Plant mucilage as a biofilm matrix that shapes the rhizosphere microbial habitat. *Frontiers in Plant Science* 12: 798992.

Newgard, C.B.J. 2026. *Metabolomics*. Encyclopedia Britannica. (https://www.britannica.com/science/metabolomics). Accessed on 29 Jan 2026.

Palama, T.L.; Khatib, A.K.; Choi, Y.H.; Payet, B.; Fock, I.; Verpoorte, R.; *et al.* 2009. Metabolic changes in different developmental stages of *Vanilla planifolia* pods. *Journal of Agricultural and Food Chemistry* 57: 7651-7658.

Pearse, A.G.E. 1985. *Histochemistry: Theoretical and Applied*. 4th ed. Churchill Livingstone, Edinburgh. 624p.

Pizzolato, T.D.; Lillie, R.D. 1973. Mayer's tannic acid–ferric chloride stain for mucins. *Journal of Histochemistry and Cytochemistry* 21: 56-64.

Reis, A.S.; Santos, A.S.; Gonçalves, J.F.C. 2021. Ultrasound-assisted lipid extractions enriched with sterols and tetranortriterpenoids from *Carapa guianensis* seeds and the application of lipidomics using GC/MS. *Royal Society of Chemistry Advances* 11: 33160-33168.

Rohman, A.; Che Man, Y.B. 2013. Application of FTIR spectroscopy for monitoring the stabilities of selected vegetable oils during thermal oxidation. *International Journal of Food Properties* 16:1594-1603.

Schaller, H. 2003. The role of sterols in plant growth and development. *Progress in Lipid Research* 42: 163-175.

Silva, T.R.; Camargo, L.E.V.; Vicintim, A.B.; Silva, A.J.R.; Simas, D.L.R. 2024. Espécies de baunilha (*Vanilla*) do Brasil com potencial valor econômico. *Revista Virtual de Química* 16: 436-444.

Silva Oliveira, J.P.; Garrett, R.; Koblitz, M.G.B.; Macedo, A.F. 2025. Integrated targeted and untargeted metabolomics profiling of *Vanilla* species from the Atlantic Forest: Unveiling the bioeconomic potential of *Vanilla cribbiana*. *Food Chemistry* 464: 141650.

Singletary, K.W. 2020. *Vanilla*: potential health benefits. *Nutrition Today* 55: 186-196.

Soto Arenas, M.A.; Cribb, P. 2010. A new infrageneric classification and synopsis of the genus *Vanilla* Plum. ex Mill. (Orchidaceae: Vanillinae). *Lankesteriana* 9: 355-398.

Stuart, B.H. 2004. *Infrared spectroscopy*: *fundamentals and applications*. John Wiley & Sons, Chichester. 242p.

Tosif, M.M.; Najda, A.; Bains, A.; Kaushik, R.; Dhull, S.B.; Chawla, P.; Walasek-Janusz, M. 2021. A Comprehensive Review on Plant-Derived Mucilage: Characterization, Functional Properties, Applications, and Its Utilization for Nanocarrier Fabrication. *Polymers* 13(7): 1066.

Toth, S. 2018. Volatile compounds in *Vanilla*. In: Havkin-Frenkel, D.; Belanger, F.C., eds. *Handbook of Vanilla Science and Technology*. Chichester: John Wiley & Sons Ltd., 285-347.

Wagner, H.M.; Bladt, S. 2009. *Plant drug analysis: A Thin Layer Chromatography Atlas*. 2nd ed. Springer-Verlag, New York. 320p.

Wörheide, M.A.; Krumsiek, J.; Kastenmüller, G.; Arnold, M. 2021. Multi-omics integration in biomedical research – A metabolomics-centric review. *Analytica Chimica Acta* 1141: 144-162.

Yu, M.; Gouvinhas, I.; Rocha, J. 2021. Phytochemical and antioxidant analysis of medicinal and food plants towards bioactive food and pharmaceutical resources. *Scientific Reports* 11: 1-14.

Yusuf, N.; Masor, N.; Zolkeflee, P.; Zakaria, N.; Wahab, N.; Asari, A.; Aziz, A. 2023. Qualitative phytochemical analysis, enzymatic and non-enzymatic antioxidant activity in stems and leaves of *Vanilla planifolia* (Orchidaceae). *Food Research* 7: 165-172.

RECEIVED: 13/10/2025
ACCEPTED: 20/05/2026
ASSOCIATE EDITOR: Waldireny Gomes

DATA AVAILABILITY: All data generated or analysed during this study are included in this published article.

AUTHOR CONTRIBUTIONS: Borges, I.T.F. - conceptualization, investigation, formal analysis, methodology, visualization, writing – original draft, writing – review and editing; **Barra, I.M.M.** - investigation, formal analysis, methodology; **Barberena, F.F.V.A.** - conceptualization, resources, writing – review and editing; Santos, A.S. - resources, writing – review and editing; **Feio, A.C.** - conceptualization, formal analysis, methodology, project administration, resources, supervision, writing – review and editing.

This is an Open Access article distributed under the terms of the Creative Commons Attribution License, which permits unrestricted use, distribution, and reproduction in any medium, provided the original work is properly cited.